Springer

KSME

Journal of Mechanical Science and Technology 27 (11) (2013) 3299~3307
www.springerlink.com/content/1738-494x
DOI 10.1007/s12206-013-0852-x

Effects of a blade profile, the Reynolds number, and the solidity on the performance of a straight bladed vertical axis wind turbine †

Sung-Cheoul Roh[1] and Seung-Hee Kang[2,*]

[1]*Department of Materials, Mechanical and Automation Engineering, Yanbian University of Science and Technology, Beishan St., Yanji City, Jilin Province, 133000, China*
[2]*Department of Aerospace Engineering, Chonbuk National University, Jeonju, 561-756, Korea*

(Manuscript Received September 14, 2012; Revised May 7, 2013; Accepted August 18, 2013)

Abstract

This study investigates the effects of parameters such as a blade profile (changing the digit of the 4-digit NACA00xx airfoil), the Reynolds number, and the solidity on the performance characteristics of a straight bladed vertical axis wind turbine (VAWT). A numerical analysis, adopting the multiple stream tube (MST) method, is carried out to evaluate the performance depending on the parameters. The numerical result shows that the variation of a blade profile directly influences the power production, i.e., the high-digit NACA00xx airfoil provides higher power in a low speed zone (BSR < 3; BSR: blade speed ratio ($\Omega R/U_f$), Ω: angular velocity of blade, R: radius of a straight Darrieus wind turbine, U_f: free stream velocity) than the low-digit NACA00xx profile. On the contrary, the low-digit NACA00xx airfoil produces higher power in a high speed range (BSR > 5) than the high-digit NACA00xx profile. An enhancement of the power production is observed with increasing the Reynolds number on the whole tested blade speed ratio range (1 < BSR < 12). In particular, the rate of the enhancement of the power is rapidly decreased with the increases of the Reynolds number ($Re = \rho \bar{U}_r c/\mu$, ρ: air density, $\bar{U}_r$: mean resultant velocity acting on a blade with variable rotating speeds in a uniform free stream velocity (U_f), c: blade chord length, μ: air viscosity). For the effect of the solidity on the power production, a marked reduction of the range of the blade speed ratio that can provide the power is observed with increasing the solidity. A pattern of very steep variation of the power around the peak in the low speed zone (BSR < 3) is found in a high solidity range ($\sigma > 0.3$; σ: solidity (Nc/R), N: number of blade, c: chord length of an airfoil), and this tendency is conspicuously different from that of the eggbeater-type Darrieus VAWT, which is interpreted as a gradual variation of the power around the peak.

Keywords: Straight-type Darrieus VAWT; Multi-stream tube method; Blade profile; Reynolds number; Solidity; Power coefficient

1. Introduction

In general, wind turbines are categorized into two major types: horizontal axis type (HAWT) and vertical axis type (VAWT) machines [1-3]. Particularly, the VAWT is divided into three basic types: Savonius type, Darrieus eggbeater type, and Darrieus straight type [2]. Fig. 1 shows the schematics of the HAWT and the VAWT.

In the past couple of decades, remarkable researches have been carried out to understand the physics of the HAWT; however, comparatively less attention has been given to the VAWT [1, 3]. Recently, because the VAWT has advantages over the HAWT, in spite of the disadvantages as shown in Table 1, considerable researches on the VAWT are being undertaken [1-7]. Also, since the Savonius type has less efficiency than the two Darrieus types, and the Darrieus straight type is much easier to fabricate and install than the Darrieus eggbeater type [2], recent researches on the VAWT are concentrated on the straight-type Darrieus wind turbine.

Deglaire et al. [6], who did a numerical study to evaluate the forces on a rotating blade of the straight type VAWT, mentioned that a blade profile is one of the key factors to affect the performance of a wind turbine. Howell et al. [1] investigated the performance of a small straight-type Darrieus wind turbine by using a wind tunnel. The results of their study illustrate that the performance of a turbine is enhanced with increasing the wind speed (increasing the Reynolds number) and decreasing the number of blades of a turbine (decreasing the solidity). Therefore, the Reynolds number and the solidity directly affect the performance of a wind turbine. Also, concerning a method to overcome the starting load of a turbine, Refs. [1, 7], mentioned that high solidity provides a high torque in low BSR and consequently improves the so called 'self-starting' of a turbine. Thus, the blade profile, Reynolds number, and solidity are important parameters to characterize the performance of the

*Corresponding author. Tel.: +82 63 270 2469, Fax.: +82 63 270 2472
E-mail address: ksh@jbnu.ac.kr
† Recommended by Associate Editor Donghyun You

Table 1. Advantages and disadvantages of VAWT over HAWT (from Refs. [1, 3, 7, 8]).

Advantages
• Low dependency on the local wind direction (need not yaw mechanism).
• Ease of the blade fabrication and the overall installation and operation.
• Durability in wind gust.
• Lower manufacturing cost.
• Lower noise.
Disadvantages
• Self-starting in a load.
• Less maximum power efficiency C_p (~0.4 (VAWT) < ~0.49 (HAWT)).

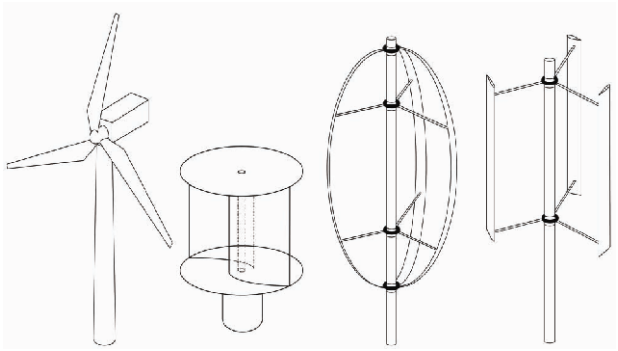

(a) (b) (c) (d)

Fig. 1. Configurations of the HAWT and the VAWT: (a) HAWT; (b) savonius type VAWT; (c) eggbeater type VAWT; (d) straight type VAWT.

straight-type Darrieus wind turbine. Therefore, it is required to assess the effects of these parameters on the performance of the straight-type Darrieus turbine in a synthetic way.

In the present study, we investigate the power behavior of a straight type VAWT, with respect to a blade profile (changing the digit of the 4-digit NACA00xx airfoil), the Reynolds number, and the solidity in detail, through a numerical method. Numerical methods for analyzing the performance of the VAWT have been classified into mainly two kinds: the computational fluid dynamics (CFD) methodology that analyzes directly the flow around the blade of a wind turbine [1, 9, 10, 11]; and the semi-empirical method of the blade element momentum (BEM) theory that adopts the lift and drag coefficients of two-dimensional airfoils obtained by a wind tunnel test [2, 12]. Present study employs the multiple stream tube method of Strickerland [13], which is one of the BEM methodologies, possessing features of being fast and correct in the numerical calculation.

The results confirm that the blade profile directly affects the performance of the straight-type Darrieus VAWT, i.e., the high-digit NACA00xx airfoil provides higher power than the low-digit NACA00xx airfoil in a low speed region (BSR < 3), while the low-digit NACA00xx airfoil provides higher power than the high-digit NACA00xx airfoil in a high speed region (BSR > 5). Moreover, the power production is enhanced in the whole tested BSR range (1 < BSR < 12) with increasing the

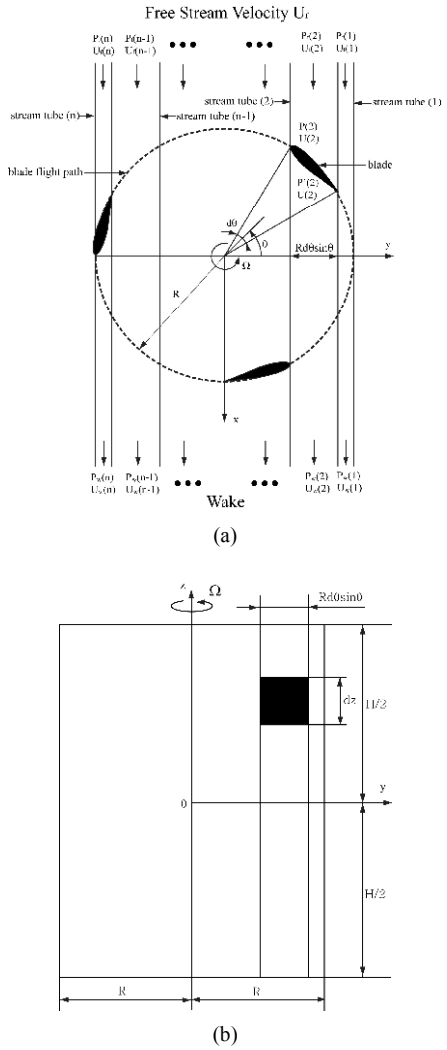

Fig. 2. Schematics for the geometric configuration of the rotating blade and its stream tube: (a) top view; (b) side view.

Reynolds number, and the rate of the enhancement is rapidly reduced with further increasing the Reynolds number. When the solidity is increased over a certain value, the power variation of the straight-type Darrieus VAWT in low BSR range is quite different from that of the eggbeater-type Darrieus VAWT, i.e., for the straight type VAWT, the pattern of the power variation around the peak is noticed to be very steep, which is contrasted to that of the eggbeater-type Darrieus wind turbine that possesses a gradual variation of the power around the peak.

2. Numerical method

Performance characteristics of a straight-type Darrieus wind turbine are evaluated through a numerical analysis using the MST method of Strickland [13]. The numerical procedure of the MST method is summarized as three steps: first, to find the force acting on a blade section at an arbitrary azimuth angle within a single stream tube (Fig. 2) using the blade ele-

ment theory and the momentum theory (blade element/momentum theory or BEMT); second, to find the torque and the power from the calculated forces, and finally to determine the total power of the turbine at an arbitrary BSR by summing up the powers of the stream tubes.

2.1 Applying the momentum theory

The streamwise average force acting on the blade section can be obtained from applying the momentum theory on the stream tube shown in Fig. 2(a) as the following equations.

$$\overline{F_x} = \rho A_s U(U_f - U_w) \tag{1}$$

$$\overline{F_x} = (p - p')A_s \tag{2}$$

where ρ is the air density, P is the air pressure in the near upstream of the airfoil, P' is the air pressure in the near downstream of the airfoil, U is the estimated average air velocity passing through the airfoil, and the subscripts f and w indicate the free stream and the wake, respectively, and A_s is the cross-sectional area of the stream tube which is defined as

$$A_s = Rd\theta \sin\theta dz \tag{3}$$

where R is the turbine radius, $d\theta$ is the projection angle of the stream tube at an arbitrary azimuth angle, and dz is the spanwise sectional length of the blade as shown in Fig. 2(b).

Applying Bernoulli's equation, between the far free stream and the near upstream of the airfoil and between the near downstream of the airfoil and the far wake as shown in Fig. 2(a), gives the following equations, respectively.

$$p_f + \frac{1}{2}\rho {U_f}^2 = p + \frac{1}{2}\rho U^2 \tag{4}$$

$$p' + \frac{1}{2}\rho U^2 = p_w + \frac{1}{2}\rho {U_w}^2. \tag{5}$$

With an assumption that the far oncoming free stream pressure P_f is equal to the wake stream pressure P_w, combining Eqs. (4) and (5) provides the following equation.

$$p - p' = \frac{1}{2}\rho({U_f}^2 - {U_w}^2). \tag{6}$$

Inserting Eq. (6) into Eqs. (1) and (2) gives

$$U = \frac{U_f + U_w}{2}. \tag{7}$$

If an interference factor *'a'* is newly defined as

$$a = \frac{U_f - U}{U_f} = 1 - \frac{U}{U_f} \tag{8}$$

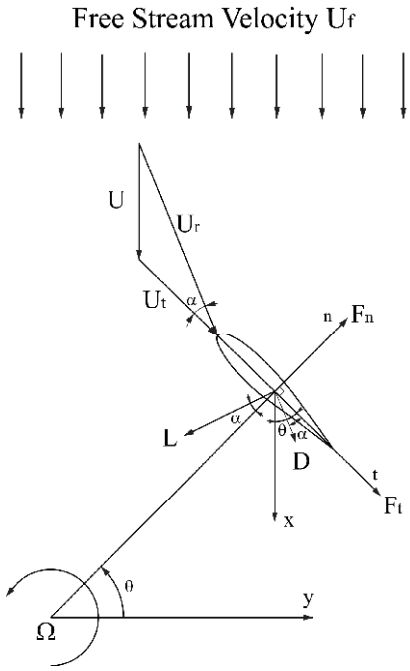

Fig. 3. Schematics of the rotating blade at an arbitrary azimuth angle θ with velocities approaching to the blade and forces acting on the blade.

and the interference factor is inserted into Eq. (7), the wake velocity U_w can be written as

$$U_w = (1 - 2a)U_f. \tag{9}$$

Substituting the wake velocity U_w into Eq. (1), the streamwise average force can be written as a function of the interference factor and the free stream velocity as

$$\overline{F_x} = 2\rho A_s(1 - a)a{U_f}^2. \tag{10}$$

2.2 Applying the blade element method

As shown in Fig. 3, the force acting on a rotating blade section at an arbitrary azimuth angle θ is divided into the tangential (F_t) and the normal (F_n) forces as

$$F_t = -\frac{1}{2}\rho C_t \delta A {U_r}^2 \tag{11}$$

$$F_n = -\frac{1}{2}\rho C_n \delta A {U_r}^2 \tag{12}$$

where δA is the plan area of a blade section ($\delta A = cdz$; c: the chord length, dz: the spanwise sectional length of the blade), C_t is the tangential force coefficient, C_n is the normal force coefficient, and U_r is the resultant velocity approaching to the blade section. The streamwise force F_x, acting on the blade section, at the azimuth angle θ is given by the tangential and normal forces (F_t and F_n) as

$$F_x = -(F_n \sin\theta - F_t \cos\theta). \tag{13}$$

If the turbine has N blades, i.e., the turbine is a multi-bladed VAWT system, the average streamwise force acting on the blade section in a single stream tube for one revolution can be obtained as

$$\overline{F_x} = NF_x \frac{2d\theta}{2\pi}. \tag{14}$$

Because the average streamwise force acting on the blade section obtained from the blade element theory must be equal to that of the momentum theory, the following equation is obtained from Eqs. (1), (7), and (14) as

$$NF_x \frac{2d\theta}{2\pi} = 2\rho A_s U(U_f - U). \tag{15}$$

Rearranging Eq. (15) with the interference factor defined in Eq. (8) gives the following equation as

$$\frac{NF_x}{2\pi\rho Rdz\sin\theta U_f^{\,2}} = \frac{U}{U_f}(1-\frac{U}{U_f}) = (1-a)a. \tag{16}$$

Combining Eqs. (11)-(13) and (16) provides the following equation.

$$\begin{aligned} a &= a^2 + \frac{NF_x}{2\pi\rho Rdz\sin\theta U_f^{\,2}} \\ &= a^2 - \frac{N}{2\pi\rho Rdz\sin\theta U_f^{\,2}}(F_n\sin\theta - F_t\cos\theta) \\ &= a^2 + \frac{Nc}{4\pi R}\left(\frac{U_r}{U_f}\right)^2 (C_n - C_t\frac{\cos\theta}{\sin\theta}) \\ &= a^2 + \frac{Nc}{4\pi R}\left(\frac{\sin\theta}{\sin\alpha}(1-a)\right)^2 (C_n - C_t\frac{\cos\theta}{\sin\theta}) \end{aligned} \tag{17}$$

where the tangential force and the normal force coefficients (C_t and C_n) can be written by the lift and the drag coefficients (C_l and C_d) and the angle of attack as

$$C_t = C_l\sin\alpha - C_d\cos\alpha \tag{18}$$

$$C_n = C_l\cos\alpha + C_d\sin\alpha \tag{19}$$

where the lift and drag coefficients (C_l and C_d) at an arbitrary angle of attack are obtained from the experimental data of Ref. [14].

Also, the relation between the resultant velocity U_r and the free stream velocity U_f can be written as a function of the interference factor a, the azimuth angle θ, and the angle of attack α as

$$\frac{U_r}{U_f} = \frac{U_r}{U}\frac{U}{U_f} = \frac{\sin\theta}{\sin\alpha}(1-a) \tag{20}$$
$$(\because U_r\sin\alpha = U\sin\theta).$$

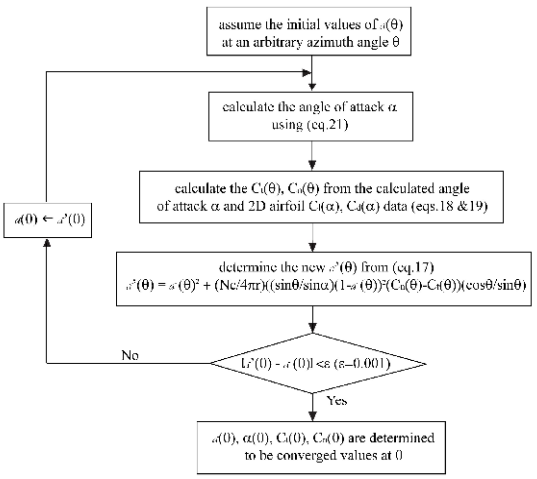

Fig. 4. Calculating procedure for the interference factor a, angle of attack α, and the force coefficients C_t and C_n at an arbitrary azimuth angle θ.

As shown in Fig. 2, the angle of attack α at a specified azimuth angle θ with an arbitrary angular speed Ω is calculated as:

$$\alpha = \tan^{-1}\left(\frac{\sin\theta}{\cos\theta + \Omega R/U}\right). \tag{21}$$

To determine the resultant velocity U_r, the angle of attack α, the interference factor a, and the tangential and normal forces coefficients (C_t and C_n) at an arbitrary azimuth angle θ, an iterative procedure using Eqs. (18)-(20) and (21) is to be required as shown in Fig. 4.

By summing up the torques obtained from each of the stream tubes, the average total torque acting on a rotational axis of the turbine at an arbitrary BSR can be calculated as

$$\overline{T} = \frac{1}{2\pi}\int_0^{2\pi}\int_{-H/2}^{H/2}\frac{1}{2}\rho RcNC_t U_r^{\,2}dzd\theta \tag{22}$$

where H is the length of blade of the turbine and N is the number of blades of the turbine.

The power of the turbine at an arbitrary angular velocity Ω is determined from multiplying the average total toque, derived from Eq. (22), by the angular velocity Ω. Then, the power coefficient C_p is obtained from dividing the calculated power by the total air flowing power passing through the cross-sectional area of the total stream tubes as

$$C_p = \frac{\overline{T}\Omega}{\frac{1}{2}\rho AU_f^{\,3}} \tag{23}$$

where A is the blade swept area ($A = 2RH$; R: the turbine radius, H: the length of a blade). In general, to represent the torque characteristics of a turbine, torque coefficient (C_Q) is

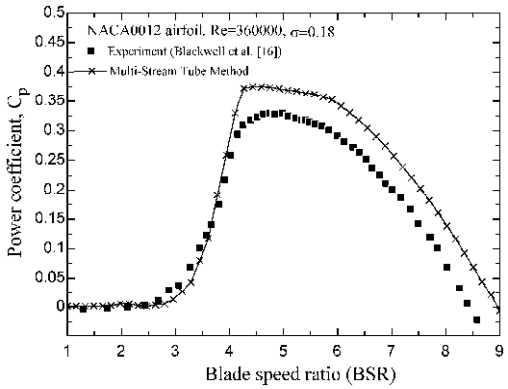

Fig. 5. Comparison of power coefficients obtained from different methods.

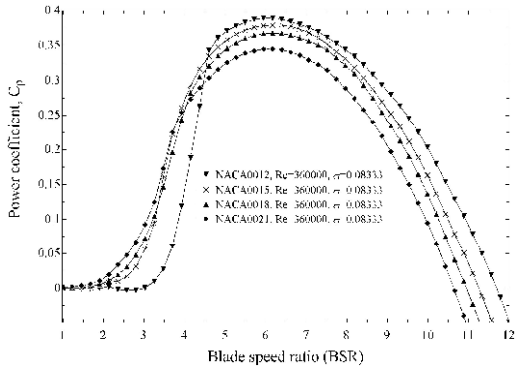

Fig. 6. Power coefficient variation with changing the blade profile.

defined as dividing the power coefficient (C_p) by the blade speed ratio (*BSR*) [15] as follows:

$$C_Q = \frac{C_p}{BSR}. \tag{24}$$

2.3 Code validation

A code that can analyze the performance of the Darrieus type wind turbine is programmed through the above mentioned numerical scheme of the MST method of Strickland [13]. An experimental result of Blackwell et al. [16], which was carried out to evaluate the performance of the Darrieus wind turbine that had a modified troposkien-type shape, was used to validate the code.

Fig. 5 shows the comparison between the numerical results using the code and the experimental data [16] at the same conditions of Re = 360,000, σ = 0.18, and the same kind of blade profile (NACA0012). As shown in Fig. 5, the calculation results using the code are appeared to be comparatively well matched together with the experimental data [16]. However, some deviations are noticed between the calculation results and the experimental data, such as higher calculation results than the experimental results in the high speed range of BSR > 4. For reducing the deviations in the range of BSR > 4, it is considerable to note that the turbulence intensity reduces the power of a turbine in high speed range [17]. However, our intent is to observe relative comparisons of the performance of the VAWT from the variations of a blade profile, the Reynolds number, and the solidity without implementing the effects of the turbulence in the MST calculation.

3. Results and discussion

3.1 Blade profile effects

To find the effects of the blade profile on the performance of a straight-type Darrieus VAWT, the four-digit symmetrical NACA airfoil profiles were selected, and the performance of the turbine was evaluated for changing the digit of the symmetrical NACA profile at a given condition of Re = 360,000 and σ = 0.08333.

Fig. 6 shows the variation of the power production according to the variation of the digit of the symmetrical NACA airfoil profile, which indicates that a blade profile directly affects the performance of the straight-type Darrieus VAWT. In particular, as noticed in the figure, there is an inflected zone of speed, where the dependency of the blade profile on the power production is inversely changed: the high-digit symmetrical NACA profile provides higher power than the low-digit symmetrical NACA profile at a low blade speed of BSR < 3; however, at a high blade speed of BSR > 5, the low-digit symmetrical NACA profile produces higher power than the high-digit symmetrical NACA profile. From this result, for the power enhancement due to the change of the blade profile, it is concluded that the high-digit symmetrical NACA airfoil is favorable in the low blade speed range of BSR < 3, while, the low-digit symmetrical NACA profile is favorable in the high blade speed range of BSR > 5.

To understand why the power production depends on a blade profile as of Fig. 6, the angle of attack at an arbitrary azimuth angle, resulting from the blade rotation and approaching free stream velocity at the azimuth angle, is delineated for the variation of a blade profile as shown in Fig. 7, and the lift force acting on the blade is represented with the variation of the blade profile and the angle of attack as shown in Fig. 8 [14]. In addition, in Fig. 7 the angle of attack varies considerably with the blade speed ratio (BSR) of the turbine, but almost not with the variation of the blade profile, i.e., at BSR = 3, the angle of attack ranges from 0^o to about 20^o according to the azimuth angle, while, at BSR = 6, the angle of attack ranges from 0^o to about 9^o. In Fig. 8, the lift coefficient is observed to be high as decreasing the digit of the symmetrical NACA airfoil profile when the range of the angle of attack is between 0^o and 9^o. But, when the angle of attack is increased over 9^o, the lift force coefficient increases with increasing the digit of the symmetrical NACA airfoil profile. Therefore, the inverse pattern of the performance of the turbine according to the changing the blade profile, observed in the speed range of 3 < BSR < 5 as shown in Fig. 6, is reasonably understood.

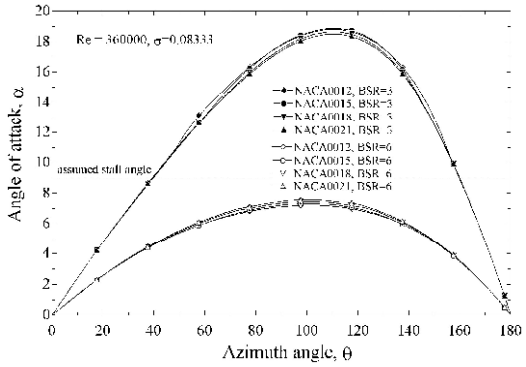

Fig. 7. Variation of the angle of attack α according to changing the blade profile at different BSRs.

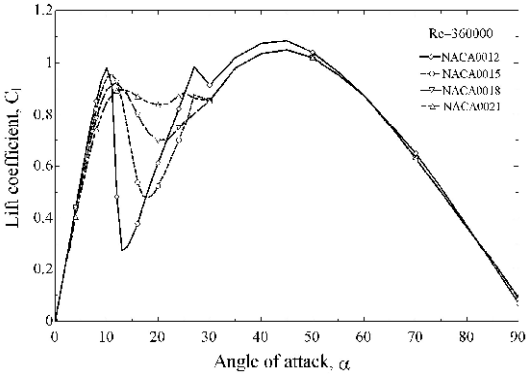

Fig. 8. Variation of the lift coefficient according to changing the blade profile (data from Ref. [14]).

3.2 Reynolds number effect

For the effects of the Reynolds number on the performance of a straight-type Darrieus VAWT, which uses the NACA0015 airfoil as a blade profile, the power according to the variation of the blade speed ratio (BSR) was calculated with the variation of the Reynolds number ($8.0 \times 10^4 \leq Re \leq 7.0 \times 10^5$) at a fixed solidity ($\sigma = 0.08333$).

Fig. 9 shows that the power production of the turbine is enhanced with increasing the Reynolds number in the overall blade speed range ($1 < BSR < 12$). The figure confirms that the Reynolds number directly affects the enhancement of the power of the straight-type Darrieus VAWT. Also, the rate of the power enhancement with the increases of the Reynolds number is reduced with approaching to a high Reynolds number. In relation to this phenomenon, Armstrong et al. [5] mentioned that the power production of a turbine will be independent of Reynolds number at an arbitrary high Reynolds number. Especially, in the low speed range of $BSR < 3$, a relatively high sensitivity of the power variation with changing the Reynolds number is noticed. The result accords closely with the expression of Kirke and Lazauskas [7] that high Reynolds number in a low operational speed range improves the 'self-starting' performance.

To comprehend the reason that the Reynolds number directly affects the power production as shown in Fig. 9, the angle of attack at an arbitrary azimuth angle is represented with the variation of the Reynolds number as shown in Fig. 10, and the lift coefficient variation according to the angle of attack is provided with varying the Reynolds number in Fig. 11 [14]. As shown in Fig. 10, the variation of the angle of attack according to the variation of the azimuth angle appears to be slightly dependent on the Reynolds number, but to be highly dependent on the blade speed ratio (BSR), i.e., in the low

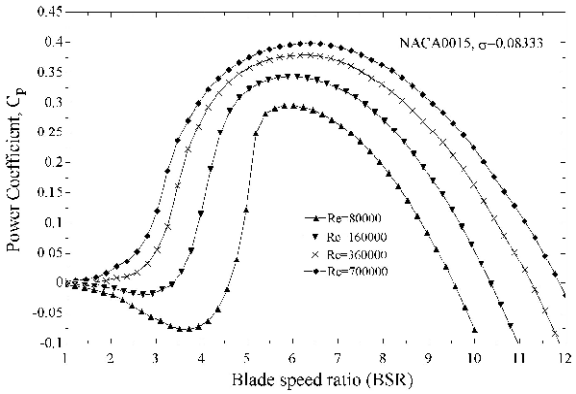

Fig. 9. Power coefficient variation with changing the Reynolds number.

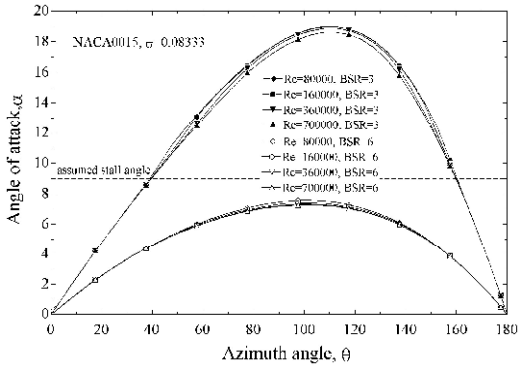

Fig. 10. Variation of the angle of attack α according to changing the Reynolds number at different BSRs.

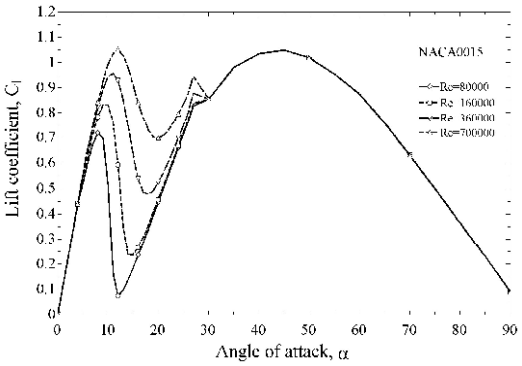

Fig. 11. Variation of the lift coefficient with changing the Reynolds number (data from Ref. [14]).

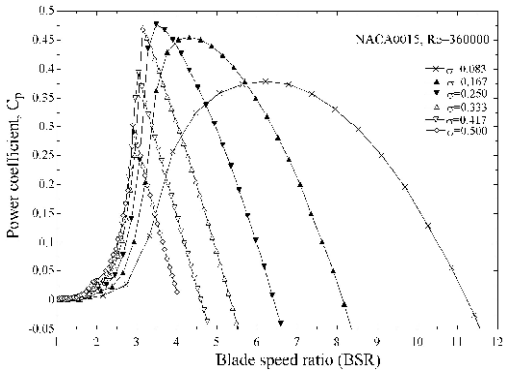

Fig. 12. Power coefficient variation with changing the solidity.

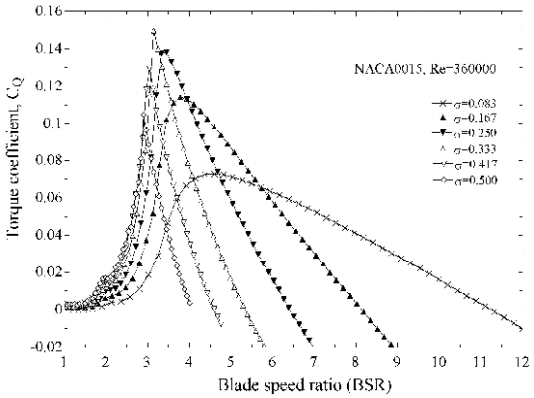

Fig. 13. Torque coefficient variation with changing the solidity.

blade speed of BSR = 3, the variation of the angle of attack according to the variation of the azimuth angle ranges from 0^o to about 20^o, while, in the high blade speed of BSR = 6, the angle of attack is from 0^o to about 9^o. As noticed in Fig. 11, when the angle of attack is about between 0^o and 20^o, the lift coefficient is directly proportional to the magnitude of the Reynolds number.

Therefore, it is reasonable that the augments of the power with increasing the Reynolds number at the blade speeds of BSR = 3 and BSR = 6 as shown in Fig. 9 are directly related to the high lift force due to the increases of the Reynolds number.

3.3 Solidity effect

For evaluating the solidity effect on the performance of a straight-type VAWT which adopts the NACA0015 airfoil as a rotating blade, the power production with the variation of the solidity ($0.08333 \leq \sigma \leq 0.5$) is calculated at Re = 360,000 as shown in Fig. 12.

A prominent power dependency on the solidity is observed as in Fig. 12. The peak power appears to be augmented with increasing the solidity till $\sigma = 0.25$; then, the peak seems to be decreased with further increasing the solidity from $\sigma = 0.25$ to $\sigma = 0.5$. Moreover, the blade speed range, in which the power can be generated, is considerably reduced with increasing the solidity. The power dependency on the solidity, shown in Fig. 12, is almost similar to that of the eggbeater-type Darrieus VAWT [13]. However, in the high solidity range ($\sigma > 0.333$), there is a considerable difference in the power variation around the peak between the straight-type and the eggbeater-type Darrieus VAWTs, i.e., the power around the peak varies in a rapid way for the straight-type Darrieus VAWT, while varying in a gradual way for the eggbeater-type Darrieus VAWT [13]. The reason for the difference in the power behavior around the peak between the two types of Darrieus VAWTs is inferred from the fact that the angle of attack along the blade span for the straight-type Darrieus VAWT is considered to be constant (see Fig. 1(d)); on the contrary, for the eggbeater-type Darrieus VAWT in which the blade is curved along the blade span (see Fig. 1(c)), the angle of attack is considered to be variant along the blade span.

Fig. 13 shows the variation of torque coefficient with changing the solidity in the same conditions as of Fig. 12. As noticed in Fig. 13, for the favor of overcoming the so called 'self-starting' problem, a salient enhancement of the torque with increasing the solidity appears in the low blade speed range (BSR < 2). As mentioned by Kirke and Lazauskas [7], since a straight-type Darrieus VAWT should overcome the starting load in the initial operation, a high torque achievement in the low blade speed range is important. Therefore, as shown in Fig. 13, the enhancement of the torque with increasing the solidity in the low speed range (BSR < 2) could be recommended as a method to overcome the 'self-starting' problem of a straight-type Darrieus VAWT, which adopts the symmetrical NACA airfoil as a blade profile. Also, it is particularly noticed in the figure that the peak of the torque is decreased with increasing the solidity ($\sigma > 0.333$), which coincides with the expression of Ref. [7] as "high solidity reduces both peak efficiency and tip speed ratio".

4. Concluding remarks

A numerical study, adopting the multiple stream tube (MST) method, was carried out to investigate the effects of a blade profile, the Reynolds number, and the solidity on the performance of a straight bladed Darrieus VAWT.

The results confirm that the blade profile directly affects the performance of the straight-type Darrieus VAWT, i.e., the high-digit symmetrical NACA profile provides higher power in the low blade speed range (BSR < 3) than the low-digit symmetrical NACA profile; in contrast, in the high speed range (BSR > 5), the low-digit symmetrical NACA profile provides higher power than the high-digit symmetrical NACA profile.

The Reynolds number appears to be an effective key factor for increasing the power production on almost the whole test speed range (1 < BSR < 12); however, a tendency of independency of

the Reynolds number on the power production is observed as the Reynolds number increases further. When the solidity is increasing over a certain value, the power behavior of the straight-type Darrieus VAWT is considerably different from that of the eggbeater-type Darrieus VAWT, i.e., a pattern of steepened behavior of the power variation around the peak appears in the straight-type Darrieus VAWT, which is conspicuously contrasted with that of the eggbeater-type Darrieus VAWT that shows a gradual variation of the power around the peak.

Acknowledgment

This research was supported by the research funds of Chonbuk National University in 2012 and the New & Renewable Energy of the Korea Institute of Energy Technology Evaluation and Planning (KETEP), grant funded by the Korea government Ministry of Knowledge Economy (20113040020010).

Nomenclature

a : Interference factor
BSR : Blade speed ratio ($\Omega R/U_f$)
c : Chord length
A : Plan area of a blade
A_S : Cross-sectional area of stream tube
C_d : Drag coefficient
C_l : Lift coefficient
C_n : Normal force coefficient
C_t : Tangential force coefficient
C_p : Power coefficient
C_Q : Torque coefficient
F_n : Normal force acting on a blade section
F_t : Tangential force acting on a blade section
F_x : Streamwise force in a stream tube
H : Length of a blade
N : Number of blades in a vertical axis wind turbine
P : Pressure in near upstream of a blade section
P' : Pressure in near downstream of a blade section
P_f : Pressure in far upstream of a blade section
P_w : Pressure in far downstream of a blade section
Re : Reynolds number ($\rho \bar{U} c/\mu$)
T : Torque acting on a turbine axis
U : Average velocity passing through a blade
U_f : Free stream velocity far upstream of a blade
U_w : Wake velocity far downstream of a blade
U_r : Resultant velocity acting on a blade
$\bar{U}_r$: Mean resultant velocity acting on a blade with variable rotating speeds

Greek letters

α : Angle of attack
ρ : Air density
θ : Azimuth angle
σ : Solidity (Nc/R)
μ : Air viscosity
Ω : Angular velocity of a vertical axis wind turbine

References

[1] R. Howel, N. Qin, J. Edwards and N. Durrani, Wind tunnel and numerical study of a small vertical axis wind turbine, *Renewable Energy*, 35 (2010) 412-422.
[2] M. Islam, D. S. K. Ting and A. Fartaj, Aerodynamic models for Darrieus-type straight-bladed vertical axis wind turbine, *Renewable and Sustainable Energy Reviews*, 12 (2008) 1087-1109.
[3] M. M. A. Bhutta, N. Hayat, A. U. Farooq, Z. Ali, S. R. Jamil and Z. Hussain, Vertical axis wind turbine – A review of various configurations and design techniques, *Renewable and Sustainable Energy Reviews*, 16 (2012) 1926-1939.
[4] J. Kjellin, F. Bülow, S. Eriksson, P. Deglaire, M. Leijon and H. Bernhoff, Power coefficient measurement on a 12 KW straight bladed vertical axis wind turbine, *Renewable Energy*, 36 (2011) 3050-3053.
[5] S. Armstrong, A. Fiedler and S. Tullis, Flow separation on a high Reynolds number, high solidity vertical axis wind turbine with straight and canted blades and canted blades with fences, *Renewable Energy*, 41 (2011) 13-22.
[6] P. Deglaire, S. Engblom, O. Ågren and H. Bernhoff, Analytical solutions for a single blade in vertical axis turbine motion in two-dimensions, *European Journal of Mechanics B/Fluids*, 28 (2009) 506-520.
[7] B. K. Kirke and L. Lazauskas, Limitations of fixed pitch Darrieus hydrokinetic turbines and the challenge of variable pitch, *Renewable Energy*, 36 (2011) 893-897.
[8] E. Hau, Wind turbines, *Springer-Verlag Berlin Heidelberg*, Germany (2006).
[9] M. R. Castelli, A. Englaro and E. Benini, The Darrieus wind turbine: Proposal for a new performance prediction model, *Energy*, 36 (2011) 4919-4934.
[10] S. V. Ghatage and J. B. Joshi, Optimisation of vertical axis wind turbine: CFD simulations and experimental measurements, *The Canadian Journal of Chemical Engineering*, 90 (2012) 1186-1201.
[11] S. H. Wang and S. H. Chen, Blade number effect for a ducted wind turbine, *Journal of Mechanical Science and Technology*, 22 (2008) 1984-1992.
[12] B. S. Kim, W. J. Kim, S. Y. Bae, J. H. Park and M. E. Kim, Aerodynamic design and performance analysis of multi-MW class wind turbine blade, *Journal of Mechanical Science and Technology*, 25 (8) (2011) 1995-2002.
[13] J. H. Strickland, The Darrieus turbine: a performance prediction model using multiple streamtubes, Sandia National Lab Report SAND75-0431, *Sandia Laboratories*, October (1975).
[14] R. E. Sheldahl and P. C. Klimas, Aerodynamic characteristics of seven symmetrical airfoil sections through 180-degree angle of attack for use in aerodynamic analysis of vertical axis wind turbine, Sandia National Lab Report SAND80-

2114, *Sandia Laboratories*, March (1981).
[15] T. Burton, D. Sharpe, N. Tenkins and E. Bossanyi, Wind energy handbook, *John Wiley & Sons Ltd*, England (2001).
[16] B. F. Blackwell, R. E. Sheldahl and L. V. Feltz, Wind tunnel performance data for the Darrieus wind turbine with NACA0012 blades, Sandia Lab Report SAND76-0130, *Sandia Laboratories* (1976).
[17] W. Rozenn, C. S. Michael, L. J. Torben and P. S. Uwe, Simulation of shear and turbulence impact on wind turbine power performance, Riso-R-1722 (EN), *Riso National Laboratory*, Denmark, January (2010).

Sung-Cheoul Roh is an Associate Professor at the Department of Materials, Mechanical, and Automation Engineering of Yanbian University of Science and Technology in China. He received the B.S. from Seoul National University in 1991, and the M.S. and the Ph.D. from Korea Advanced Institute of Science and Technology (KAIST) in 1993 and in 2002, respectively, all in Mechanical Engineering. His recent interests are in wind turbine blade aerodynamics and enhancing the efficiency of solar energy system.

Seung-Hee Kang received the B.S. and M.S. from Korea Aerospace University in 1988 and 1991, respectively, and the Ph.D. from KAIST in 2005, all in Aerospace Engineering. He is an Associate Professor at the Department of Aerospace Engineering, Chonbuk National University. His current interests include numerical simulation, wind turbine blade, and wind tunnel testing.